Supplemental material to this article can be found at:
http://dmd.aspetjournals.org/content/suppl/2020/07/28/dmd.120.000025.DC1

1521-009X/48/10/1074–1083$35.00
DRUG METABOLISM AND DISPOSITION

https://doi.org/10.1124/dmd.120.000025
Drug Metab Dispos 48:1074–1083, October 2020

Special Section on Natural Products: Experimental Approaches to Elucidate Disposition Mechanisms and Predict Pharmacokinetic Drug Interactions

Organic Cation Transporter 1 and 3 Contribute to the High Accumulation of Dehydrocorydaline in the Heart[S]

Yingchun Chen, Cui Li, Yaodong Yi, Weijuan Du, Huidi Jiang, Su Zeng, and Hui Zhou

Laboratory of Pharmaceutical Analysis and Drug Metabolism, College of Pharmaceutical Sciences, Zhejiang University, Hangzhou, China

Received March 20, 2020; accepted July 16, 2020

ABSTRACT

Dehydrocorydaline (DHC), one of the main active components of *Corydalis yanhusuo*, is an important remedy for the treatment of coronary heart disease. Our previous study revealed a higher unbound concentration of DHC in the heart than plasma of mice after oral administration of *C. yanhusuo* extract or DHC, but the underlying uptake mechanism remains unelucidated. In our investigations, we studied the transport mechanism of DHC in transgenic cells, primary neonatal rat cardiomyocytes, and animal experiments. Using quantitative real-time polymerase chain reaction and Western blotting, we found that uptake transporters expressed in the mouse heart include organic cation transporter 1/3 (OCT1/3) and carnitine/organic cation transporter 1/2 (OCTN1/2). The accumulation experiments in transfected cells showed that DHC was a substrate of OCT1 and OCT3, with K_m of 11.29 ± 3.3 and 8.96 ± 3.7 μM, respectively, but not a substrate of OCTN1/2. Additionally, a higher efflux level (1.71-fold of MDCK-mock) of DHC was observed in MDCK-MDR1 cells than in MDCK-mock cells. Therefore, DHC is a weak substrate for MDR1. Studies using primary neonatal rat cardiomyocytes showed that OCT1/3 inhibitors (quinidine, decynium-22, and levo-tetrahydropalmatine) prevented the accumulation of DHC, whereas OCTN2 inhibitors (mildronate and l-carnitine) did not affect its accumulation. Moreover, the coadministration of OCT1/3 inhibitors (levo-tetrahydropalmatine, THP) decreased the concentration of DHC in the mouse heart. Based on these findings, DHC may be accumulated partly by OCT1/3 transporters and excreted by MDR1 in the heart. THP could alter the distribution of DHC in the mouse heart.

SIGNIFICANCE STATEMENT

We reported the cardiac transport mechanism of dehydrocorydaline, highly distributed to the heart after oral administration of *Corydalis yanhusuo* extract or dehydrocorydaline only. Dehydrocorydaline (an OCT1/3 and MDR1 substrate) accumulation in primary cardiomyocytes may be related to the transport activity of OCT1/3. This ability, hampered by selective inhibitors (levo-tetrahydropalmatine, an inhibitor of OCT1/3), causes a nearly 40% reduction in exposure of the heart to dehydrocorydaline. These results suggest that OCT1/3 may contribute to the uptake of dehydrocorydaline in the heart.

Introduction

Dehydrocorydaline (DHC) is one of the main active alkaloids in *C. yanhusuo*, an important traditional remedy used for the treatment of cardiovascular diseases and analgesia (Huang et al., 2010; Wei et al., 2017; Liu et al., 2019). DHC constitutes 8%–10% of the total alkaloids (Wu et al., 2014), and when employed in the treatment of myocardial ischemia-reperfusion injury, it dilates the coronary arteries and reduces oxygen consumption (Iranshahy et al., 2014; Yang et al., 2014; Tan et al., 2019). The protective effect of DHC on myocardial ischemia-reperfusion injury may be mediated by reducing the incidence of anoxia reperfusion arrhythmia, prolonging the duration of sinus rhythms and inhibiting the release of lactate dehydrogenase from cardiomyocytes (Zhao et al., 2003; Li et al., 2010). In addition, the inhibition of myocardial ischemia by DHC may be related to the inhibition of plasma endothelin I activity, antioxidant-free radical damage, superoxide dismutase, and glutathione peroxidase (Grube et al., 2011).

According to pharmacokinetics, DHC is widely distributed in various tissues of the body, with the highest concentration in the liver (Dou et al.,

This work was supported by the Zhejiang Provincial Natural Science Foundation of China [Grant LY19H310005] and the National Natural Science Foundation of China [Grant 81673504, 81872929].

All authors declare that there are no conflicts of interest.

https://doi.org/10.1124/dmd.120.000025.

[S]This article has supplemental material available at dmd.aspetjournals.org.

ABBREVIATIONS: DHC, dehydrocorydaline; DMEM, Dulbecco's modified Eagle's medium; GAPDH, glyceradehyde-3-phosphate dehydrogenase; HBSS, Hanks' balanced salt solution; $K_{p,uu}$, ratio of free tissue drug concentration to free plasma drug concentration at steady state; L-Car, l-carnitine; LC-MS/MS, liquid chromatography–tandem mass spectrometry; MDCK, Madin-Darby canine kidney; MDR1, multidrug resistance protein 1; MPP^+, 1-methy1-4-phenylpyridinium; OCT, organic cation transporter; OCTN, carnitine/organic cation transporter; P_{app}, apparent permeability coefficient; PB, protein binding; PMAT, plasma membrane monoamine transporter; qRT-PCR, quantitative reverse-transcription polymerase chain reaction; THP, levo-tetrahydropalmatine.

2012). Furthermore, previous tissue distribution experiments of *C. yanhusuo* alkaloids in our laboratory showed a higher concentration of DHC in the liver, kidney, and heart. Radiometry and autoradiography revealed that DHC was subjected to the first-pass effect in the liver and was mainly distributed in the liver and kidney after oral administration of ^{14}C-dehydrocorydaline to rats (Fujii et al., 1984). Metabolite analysis suggested that DHC was metabolized by O-demethylation, followed by glucuronidation or sulfation (Fujii et al., 1984; Guan et al., 2017), but the metabolic enzymes of DHC have not yet been elucidated.

The Free Drug Hypothesis states that drug molecules bind to proteins and lipids in the blood and tissues, leaving only the free drug concentration at the site of action for target engagement (Smith et al., 2010; Zhang et al., 2019). As direct measurement of the free drug concentration is challenging, it is typically obtained indirectly by measuring the protein binding and total drug concentration. The ratio of free tissue drug concentration to free plasma drug concentration at steady state ($K_{p,uu}$) will equal 1 when the drug is only in the presence of passive diffusion. Alternatively, when metabolism or transport is involved in tissue distribution of the drug, $K_{p,uu} \neq 1$.

The chemical structure of the DHC is shown in Fig. 1. The log *P* value of DHC at pH 5.5 is −0.71 (Iranshahy et al., 2014). DHC generally exists as an organic cation under physiologic conditions and is similar in structure to several quaternary alkaloids, such as coptisine and berberine, which are substrates of organic cation transporter 1/3 (OCT1/3) (Li et al., 2016). Therefore, we speculated that transporters might play an important role in determining DHC distribution in the heart.

Previous studies have reported that uptake transporters, including OCT3, carnitine/organic cation transporter 1/2 (OCTN1/2), plasma membrane monoamine transporter (PMAT), and organic anion transporting polypeptides, are expressed in the human heart (Klaassen and Aleksunes, 2010; Solbach et al., 2011; Hausner et al., 2019). However, there are no reports of studies on OCT1 protein expression in the heart. Efflux transporters are also potentially important factors that modify the cardiac concentration of drugs. Transporters are not only important carriers but also may be important participants in heart disease (Koepsell, 2020), having drug target potentials (Yang et al., 2007; Solbach et al., 2011).

Based on the expression of cardiac transporters and the structural characteristics of DHC, this study aimed to investigate and clarify the underlying accumulation mechanisms of DHC in the heart.

Materials and Methods

Materials

Dehydrocorydaline (PubChem CID: 34781; purity ≥98%) was purchased from Nanjing Guangrun Biologic Products Co., Ltd. (Nanjing, China). *C. yanhusuo* extract [T151202; high-pressure liquid chromatography with diode-array detection (HPLC-DAD) chromatogram presented in Supplemental Fig. 1] was kindly supported by Zhejiang Conba Pharmaceutical Co., Ltd. (Hangzhou, China). Levo-tetrahydropalmatine (THP), l-carnitine (L-Car), and quinidine were purchased from Aladdin Biochemical Technology Co., Ltd. (Shanghai, China). MPP^+ (1-methy1-4-phenlpyridinium), 5-bromodeoxyuracil, loratadine, decynium-22, collagenase I, and rhodamine 123 were obtained from Sigma-Aldrich (St. Louis, MO). Verapamil hydrochloride was purchased from the National Institutes for Food and Drug Control (Beijing, China). Dulbecco's modified Eagle's medium (DMEM), DMEM-F12, FBS, and trypsin were purchased from Thermo Fisher Scientific (Waltham, MA). RIPA lysis buffer, loading buffer, primary antibody dilution buffer, and BCA protein assay kits were purchased from Beyotime Institute of Biotechnology (Nanjing, China). Antibodies against OCT1 (species reactivity: human, mouse, and rat; catalog number ab178869; 76 kDa) and PMAT (species reactivity: human and rat; catalog number ab56554; 58 kDa) were purchased from Abcam (Cambridge, MA). Antibodies against OCT3 (species reactivity: human, mouse, and rat; catalog number TA322212S; 61 kDa) were obtained from Origene Technologies Inc. (Rockville, MD). Antibodies against OCTN1 (species reactivity: human, mouse, and rat; catalog number ab9739-050; 62 kDa), glyceradehyde-3-phosphate dehydrogenase (GAPDH) antibody, and the anti-rabbit and anti-mouse secondary antibodies were obtained from Multi Sciences (Lianke) Biotech Co., Ltd. (Hangzhou, China). Antibodies against OCTN2 (species reactivity: human, mouse, and rat; catalog number SAB4300885; 65 kDa) were obtained from Sigma-Aldrich. Other chemicals or solvents were the analytical reagent grade available commercially.

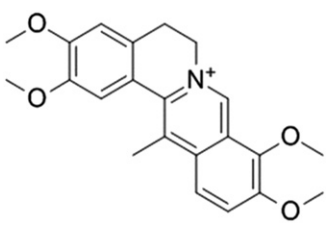

Fig. 1. The chemical structure of DHC.

Ultrafiltration Protein Binding Studies

The protein binding (PB) of DHC was determined by an ultrafiltration method, with minor modifications (Kamal et al., 2009).

Plasma Protein Binding Studies. Blank mice plasma (6–8 weeks, male) was spiked with DHC to produce 0.1, 1, and 10 μM concentrations. A 0.3-ml aliquot of each standard was added to a disposable Microcon YMT-30 centrifugal filter device (Millipore, Billerica, MA) by using an anisotropic hydrophilic membrane that excluded molecules greater than 30 kDa. The device was capped and centrifuged at 1800*g* for 25 minutes at 37°C. The protein-free ultrafiltrate was collected for each sample, the remaining plasma in the ultrafiltration tube was discarded, and the tube was rinsed 10 times with pure water. The filter membrane with acetonitrile was repeatedly rinsed thrice. The nonspecific binding rate of DHC was calculated by measuring the quantity of DHC in the mixed membrane washing liquid acetonitrile. The unbound fraction in the plasma was calculated as the ratio of DHC concentration in the ultrafiltrate to that in the original plasma standard. Liquid chromatography–tandem mass spectrometry (LC-MS/MS) was used to determine the quantity of DHC in the samples.

Heart Tissue Protein Binding Studies. One gram of heart tissue obtained from 6- to 8-week-old male mice was homogenized with 4 ml of solvent (distilled water). The blank heart homogenate was spiked with DHC to produce 0.1, 1, and 10 μM concentrations. Other steps are the same as in the plasma protein binding studies. LC-MS/MS was used to determine the quantity of DHC in the samples.

Animals

Male Institute of Cancer Research (ICR) mice (weighing 18–20 g, 6–8 weeks) were purchased from the Experimental Animal Center of the Zhejiang Academy of Medical Sciences (certificate number SCXK 2019-0002; Hangzhou, China) and housed in Zhejiang University Laboratory Animal Center. The animals were housed in cages at a controlled temperature (22.0 ± 1°C) and humidity (50%–60%) with a 12-hour light/dark cycle and free access to food and water throughout the day. The studies were approved by the Institutional Animal Care and Use Committee of Zhejiang University (No. 12626). All animal procedures were performed in accordance with the Public Health Service *Policy on Humane Care and Use of Laboratory Animals* (http://grants1.nih.gov/grants/olaw/references/phspol.htm).

Tissue distribution experiments were performed according to a preset plan, and the sample sizes did not change during the experiments. Mice were randomly allocated to six groups (eight mice each) and allowed to acclimate to the facilities for a week before being made to fast, with free access to water for 12 hours before the experiments. *C. yanhusuo* extract (1.75 $g \cdot kg^{-1}$) group and DHC (25 $mg \cdot kg^{-1}$) group had the same dosage of DHC. The extract and DHC were suspended in 0.5% aqueous solution of carboxymethyl cellulose sodium and were administered to the mice by gavage. Blood and hearts were collected 15, 30, and 60 minutes after treatment. Plasma was collected immediately after centrifugation at 8000*g* for 10 minutes. All samples were stored at −80°C until further analysis.

The effect of THP on the cardiac uptake of DHC was explored according to a preset plan. Eighteen male mice were randomly assigned to two groups (nine mice each) for the study. DHC (0.6 mg/ml) or THP (2 mg/ml) was formulated by dissolving either of them in 0.1% DMSO, 5% Solutol HS-15, 2.5% absolute ethanol, and physiologic saline, and then the solution was properly mixed. The

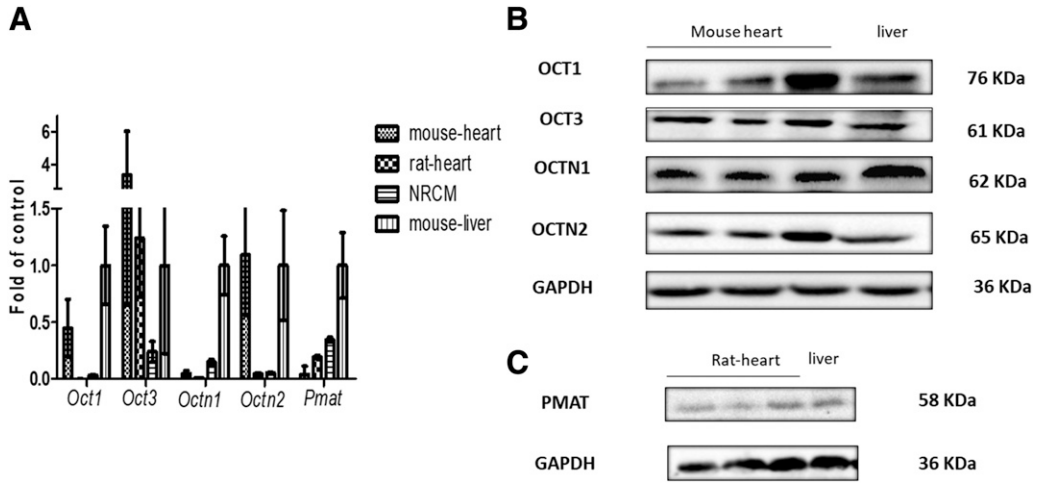

Fig. 2. *Oct1*, *Oct3*, *Octn1*, *Octn2*, and *PMAT* expression in mouse or rat heart. The mRNA expression levels of *Oct1*, *Oct3*, *Octn1*, *Octn2*, and *PMAT* in the mouse and rat heart, primary neonatal rat cardiomyocytes, and mouse liver are shown (A). Data are presented as means ± S.D., $n = 6$. The corresponding transporters expressed in the mouse liver were used as positive control. The protein expression levels of OCT1, OCT3, OCTN1, and OCTN2 in the mouse heart (B) and PMAT in the rat heart (C) are shown. The mouse or rat liver served as a positive control.

control group was treated with a single tail vein injection of DHC at a dose of 6 mg·kg^{-1}. In the THP group, THP (15 mg·kg^{-1}) and DHC (6 mg·kg^{-1}) were administered at the same time. Blood and tissues were collected 15 minutes after administration. All samples were collected and stored at −80°C until further analysis.

Real-Time Reverse-Transcription Polymerase Chain Reaction

Total RNAs were extracted from tissues ($n = 6$) and primary cells ($n = 6$) by using the RNA simple Total RNA kit (DP419; Tiangen Biotech Co., Ltd., Beijing, China). Then, cDNAs were synthesized using a PrimeScript RT reagent kit (Takara, Tokyo, Japan). The amplification reactions were detected with a StepOne plus real-time PCR system using SYBR Premix Ex Taq II (Takara). Relative expression of the target mRNAs was normalized to the housekeeping gene GAPDH. The ΔCt method was used to calculate the result, described as $2^{-\Delta Ct}$, $\Delta Ct = Ct_{target} - Ct_{GAPDH}$. Relative expression of a target gene was expressed as a fold of control, which was calculated using the following equation: fold of control = $2^{-\Delta\Delta Ct}$, where $\Delta\Delta Ct = \Delta Ct_{(sample)} - \Delta Ct_{(control)}$. The specific primers for qRT-PCR are listed in Supplemental Table 1.

Western Blot Assay

Heart tissues were lysed in RIPA lysis buffer (Beyotime Biotechnology) containing protease inhibitors, and protein concentrations were measured using BCA protein assay kits (Beyotime Biotechnology). After mixing the samples with loading buffer (P0015; Beyotime Biotechnology) and boiling at 100°C for 10 minutes, protein extracts (50 μg) from each sample were separated using SDS-PAGE (Bio-Rad, Hercules, CA) and transferred to polyvinylidene fluoride membranes (Millipore, Burlington, MA). The membranes were blocked with 5% skim milk and then incubated with one of the following primary antibodies with the primary antibody dilution buffer overnight at 4°C: anti-OCT1 (1:1000), anti-OCT3 (1:1000), anti-OCTN1 antibody (1:1000), anti-OCTN2 antibody (1:1000), anti-PMAT (1:1000), or anti-GAPDH antibody (1:5000). On the next day, membranes were washed six times with Tris-buffered saline/Tween 20 and incubated with the secondary antibody (1:5000) for 2 hours at room temperature. After six washes with Tris-buffered saline/Tween 20, membranes were visualized using the enhanced chemiluminescence kit and G-BOX Chemiluminescence Imager (LI-COR, Lincoln, NE).

Cell Culture

Madin-Darby canine kidney (MDCK) cells were obtained from Peking Union Medical College (Beijing, China). The cells were stably transfected with the full-length hOCTN1 cDNA (MDCK-hOCTN1, GenBank accession number NM_003059.2), hOCTN2 cDNA (MDCK-hOCTN2, NM_003060.3), hOCT1 cDNA (MDCK-hOCT1, NM_003057), hOCT3 cDNA (MDCK-hOCT3, NM_021977.3), and hMDR1 cDNA (MDCK-hMDR1), established by our research team (Tu et al., 2013; Sun et al., 2014, 2019; Weng et al., 2016). The mRNA expression, protein expression, and function of MDCK-hMDR1 cells were confirmed by qRT-PCR, Western blotting, and uptake study. The functional verification of transgenic cells is shown in Supplemental Fig. 2. We used MPP^+ as the positive control of OCT1/3, ergothioneine as OCTN1's positive control, L-car as OCTN2's positive control, Serotonin as PMAT positive control, and Rho123 as MDR1's positive control.

MDCK cells were cultured in DMEM supplemented with 10% FBS and 100 U·ml^{-1} penicillin-streptomycin at 37°C in a humidified atmosphere containing 5% CO_2. Primary neonatal rat cardiomyocytes were cultured in DMEM-F12 supplemented with 10% FBS, 100 U·ml^{-1} penicillin, and streptomycin in a humidified 5% CO_2 atmospheric air at 37°C.

Cellular Experiments

MDCK cells stably overexpressing human transporters and vector control cells were seeded in 24-well plates at a density of 2×10^5 cells per well. Accumulation studies were performed after 3 days of cell culture using the methods developed by our research team (Bai et al., 2017; Ma et al., 2017). The medium was removed and the cells were washed twice with Hanks' balanced salt solution (HBSS), preincubated at 37°C for 10 minutes, to determine whether DHC is the substrate of OCT1, OCT3, OCTN1, OCTN2, and PMAT. The accumulation of DHC was initiated by adding HBSS containing DHC in a range of concentrations with or without inhibitors. Quinidine is an inhibitor of OCT1 and OCTN1 (Li et al., 2014); decynium-22 is an inhibitor of OCT1/3 and PMAT (Koepsell et al., 2007; Fraser-Spears et al., 2019); THP is an inhibitor of OCT1/3 (Tu et al., 2013; Li et al., 2014) and MDR1 (Sun et al., 2012); verapamil is an inhibitor of OCT1/3 (Solbach et al., 2011; Bexten et al., 2015), OCTN1 (Koepsell et al., 2007), and MDR1 (Zhang and Benet, 1998); and meldonium and L-Car are inhibitors of OCTN2 (Koepsell et al., 2007; Dambrova et al., 2013) (Supplemental Table 2). The uptake procedure was allowed for 3 minutes and stopped by removing the incubation buffer and quickly adding ice-cold buffer (PBS: 135 mM NaCl, 2.7 mM KCl, 1.5 mM KH_2PO_4, and 8 mM K_2HPO_4, pH 7.2) at the indicated time points. Then, the cells were washed three times with ice-cold buffer (PBS) and lysed with 100 μl of 0.1% SDS.

The methods used for the assessment of DHC accumulation in primary neonatal rat cardiomyocytes at 4°C or 37°C were the same as those used in the MDCK cells.

Cell experimental results were collected and analyzed from the last two independent in vitro experiments performed in triplicate according to a preset plan.

Permeability Assays

MDCK-mock and MDCK-MDR1 cells were seeded on Transwell clear polyester membrane inserts (Corning Coster Corp., Acton, MA) in 12-well plates at a density of 2×10^6 cells per well. The medium was changed every 2 days, and cell monolayers were ready for experiments from 5 to 7 days after seeding. Trans-epithelial electrical resistance values, measured by the Millicell-ERS Voltohmmeter (Millipore Corp.), were required to exceed 200 Ω/cm^2 to ensure the integrity of the

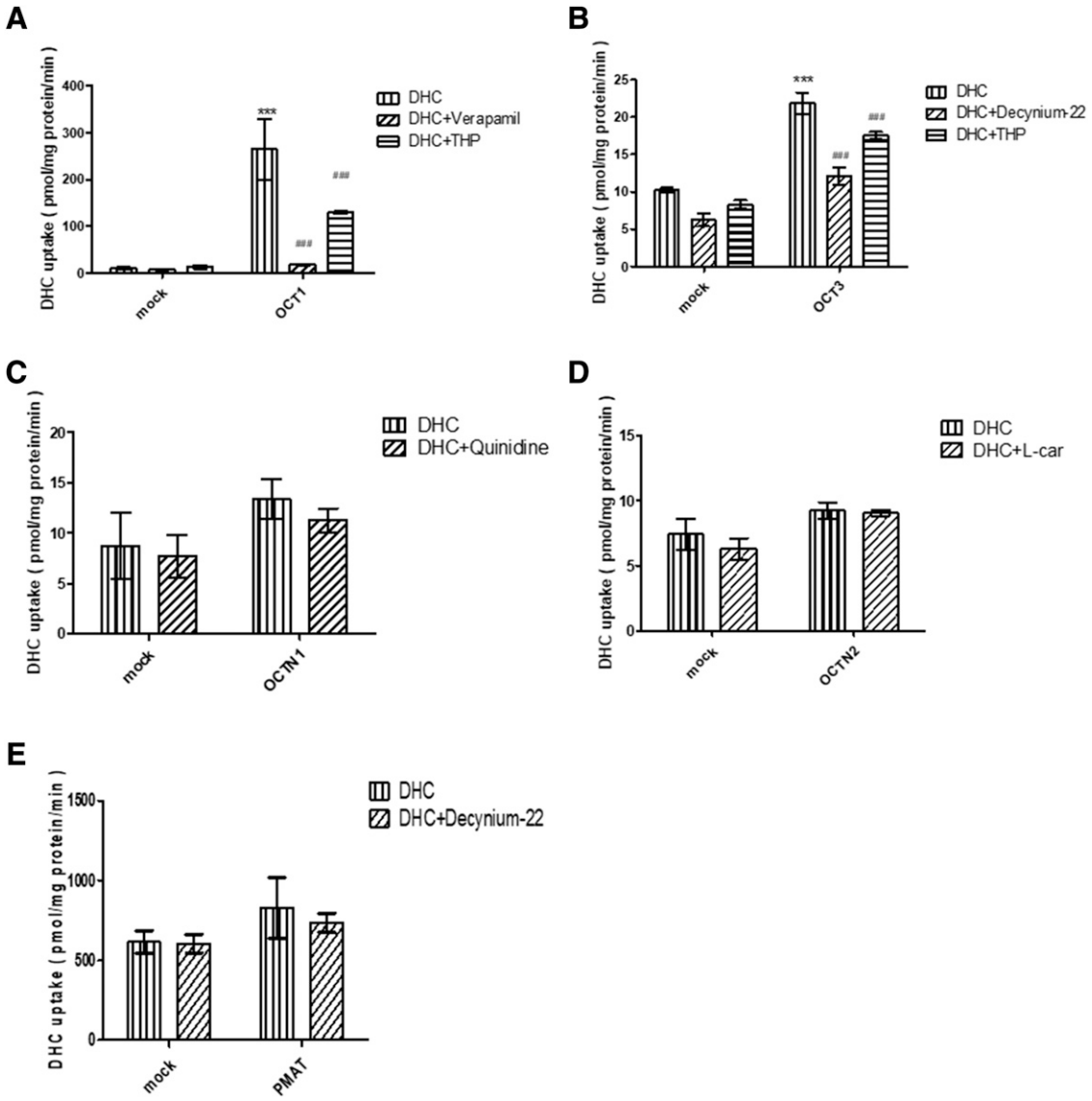

Fig. 3. DHC is a substrate of OCT1 and OCT3 but not OCTN1, OCTN2, and PMAT. Accumulation of DHC (5 μM) in MDCK-hOCT1 (A), MDCK-hOCT3 (B), MDCK-hOCTN1 (C), MDCK-hOCTN2 (D), MDCK-hPMAT (E), and MDCK-mock cells cultured in the absence or presence of typical inhibitors (OCT1: 100 μM verapamil and 10 μM THP; OCT3: 10 μM decynium-22 and 10 μM THP; OCTN1: 100 μM quinidine; OCTN2: 100 μM L-car; and PMAT: 10 μM decynium-22). Data are presented as means ± S.D., $n = 3$. Compared with the accumulation in mock cells, $^{***}P < 0.001$; compared with the accumulation in cells treated without inhibitors, $^{\#\#}P < 0.01$; $^{\#\#\#}P < 0.001$.

monolayer during the whole experiment. Simultaneously, the apparent permeability coefficient (P_{app}) of lucifer yellow must be less than 0.5×10^{-6} cm/s. The monolayers of MDCK-mock and MDCK-MDR1 cells were washed three times with HBSS and preincubated with or without verapamil (100 μM), the MDR1 inhibitor, for 30 minutes at 37°C. Transport studies were initiated by loading the DHC or rhodamine 123 HBSS solution into the donor compartment. Samples (100 μl) were removed from the receiver compartment at 10, 20, 30, 60, and 120 minutes after loading, and fresh transport medium was immediately added to replenish the wells.

The concentrations of rhodamine 123 (excitation wavelength [λ_{ex}], 485 nm; emission wavelength [λ_{em}], 535 nm) were measured using a microplate reader (Molecular Devices Corporation, Sunnyvale, CA). The concentrations of DHC were determined using LC-MS/MS.

The P_{app} was used as a transport index and was determined as $P_{app} = dQ/(dt \cdot A \cdot C_0)$, where dQ/dt is the linear appearance rate of mass in the receiver compartment during sink conditions, A is the surface area of the monolayer, and C_0 is the initial donor concentration. The efflux rate (ER) was determined using the following equation: efflux ratio = $P_{app\ (BL\text{-}AP)}/P_{app\ (AP\text{-}BL)}$. $P_{app\ (BL\text{-}AP)}$ is the P_{app} in the secretory direction from the basolateral side to the apical side. $P_{app\ (AP\text{-}BL)}$ is P_{app} in the absorptive direction from the apical side to the basolateral side.

Isolation of Primary Neonatal Rat Cardiomyocytes

Methods for isolating cardiomyocytes have improved, according to the literature (Vandergriff et al., 2015). Primary neonatal rat cardiomyocytes are generally isolated from rats that are 1–3 days old, but the sex is unknown. After the neonatal rats were disinfected with 75% alcohol, the heart was quickly removed, and the ventricle was excised. The solution of chopped ventricular tissue was transferred to a new tube and digested with 0.05% collagenase I and 0.03% trypsin. The obtained cells were cultured in DMEM-F12 at 37°C in a 5% CO_2 incubator for 1.5 hours, and then the unattached cardiomyocytes were transferred to a new culture dish. 5-Bromodeoxyuracil was added at concentration of 0.1 mM to inhibit the proliferation of fibroblasts, and the medium replaced with fresh medium after 48 hours. The cardiomyocytes gradually protruded from the pseudopod and exhibited irregular shapes, such as triangles and polygons, interwoven into a network.

Sample Processing and Quantitative Determination Using LC-MS/MS

The LC-MS/MS method for analyzing DHC has been described in our previous report (Du et al., 2018).

The cell lysate (60 μl) was mixed with 180 μl of acetonitrile containing the internal standard (100 $ng \cdot ml^{-1}$ loratadine). The mixture was vortexed for

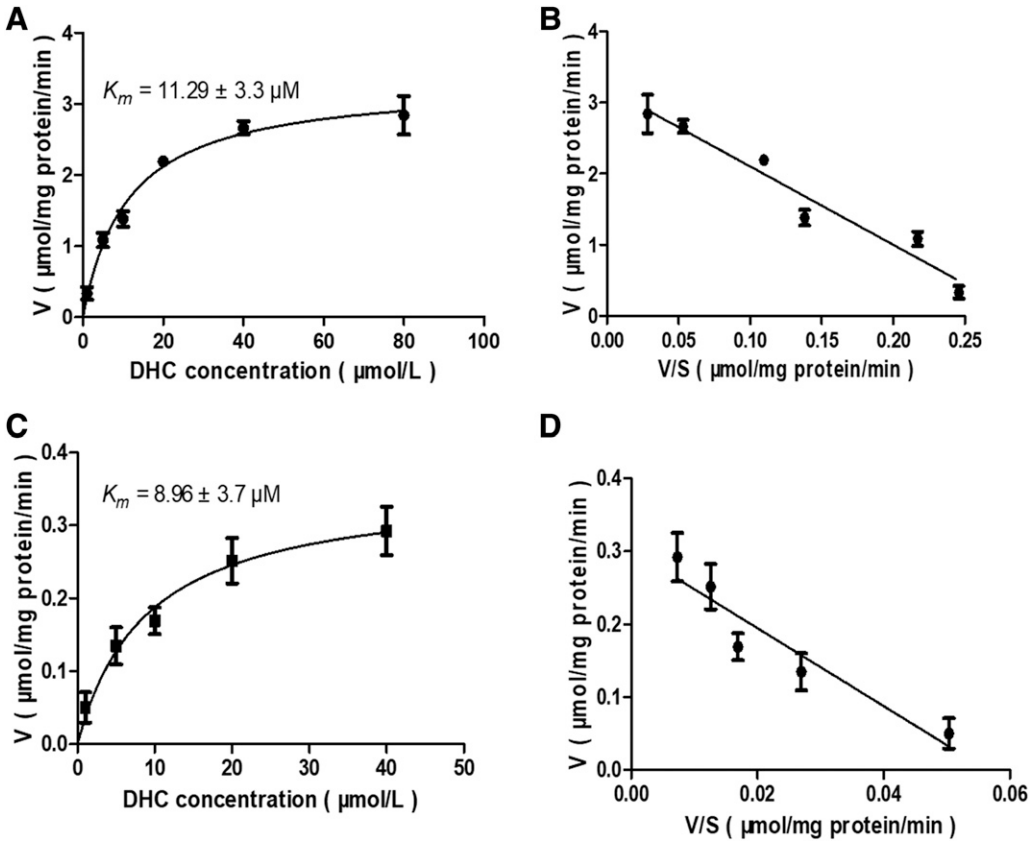

Fig. 4. The typical dynamics of DHC in MDCK-hOCT1 and MDCK-hOCT3 cells are shown. Concentration-dependent profiles of DHC uptake in MDCK-hOCT1 (A) and MDCK-hOCT3 (C) cells are shown. Uptake in MDCK-hOCT1 (B) and MDCK-hOCT3 (D) cells was analyzed by constructing an Eadie–Hofstee plot. MDCK-hOCT1, MDCK-hOCT3, and mock cells were incubated with increasing concentrations of DHC for 3 minutes at 37°C. Data are presented as means ± S.D., $n = 3$.

5 minutes and centrifuged at 13,000 rpm for 15 minutes. The supernatant was transferred to an autosampler vial, and an aliquot of 5 μl was injected into the Agilent 1290/6460 LC–MS/MS system with a triple quadrupole mass spectrometer (Agilent Technologies, Santa Clara, CA) for analysis.

Tissue samples were removed from −80°C storage and homogenized with 0.8 ml acetonitrile/water mixed liquor (75:25, v/v) for 4 minutes. Then, 200 μl homogenate was vortexed with 500 μl of acetonitrile/acetone (90:10, v/v) internal standard (100 ng·ml^{-1} loratadine) for 6 minutes. The mixture was then centrifuged at 13,000 rpm for 15 minutes. Then, 500 μl of supernatant was transferred to another Eppendorf tube and volatilized to dryness at 40°C with a vacuum concentrator system (LABCONCO, Kansas City, MO). The residue was reconstituted in 100 μl of acetonitrile/water (30:70, v/v) containing 0.1% formic acid by vortexing for 6 minutes and centrifuged at 13,000 rpm for 15 minutes. The supernatant was transferred to an autosampler vial, and an aliquot of 5 μl was injected for analysis.

DHC was quantified by Agilent 1290/6460 LC-MS/MS for all transport experiments. Chromatographic separation was performed on a ZORBAX Eclipse plus-C18 column (2.1 × 50 mm, 3.5 μm; Agilent Technologies) maintained at 35°C, with a flow rate of 0.2 ml/min. Mass spectrometry analysis was performed using an electrospray ionization (ESI) source in positive ion mode and the ion pair DHC at *m/z* 366.1→350.1 and loratadine at *m/z* 383.1→267.1. Assays used to determine the DHC concentration were validated according to the US Food and Drug Administration guidelines, and all items met these requirements.

Data Analysis

According to the Michaelis–Menten equation $V = V_{max}/(1 + (K_m/[S]))$, the Michaelis–Menten constant V_{max} and K_m (Fig. 4) were obtained using GraphPad Prism 5.0 software (GraphPad Software Inc., San Diego, CA), where V is the absorption rate and S is the substrate concentration. The specific calculation method is consistent with the literature (Yu et al., 2013; Zeng et al., 2019). Kinetic studies were performed with a series concentration of DHC after 3-minute incubation, and the background counts of mock-transfected cells were subtracted from the data. Protein binding was determined as the protein binding (%) = $1 - C_f/C_t \times (1 + P\%)$, where C_f is the free concentration, C_t is the total concentration, and P% is the nonspecific binding of the centrifugal ultrafiltration device. Data are reported as means ± S.D. from at least two independent in vitro experiments performed in triplicate ($n = 3$). An unpaired Student's *t* test was used to compare the differences between two groups (Fig. 6), and one-way ANOVA followed by Dunnett's multiple comparison post hoc test was used to evaluate the statistical significance of differences among groups (Figs. 3 and 5). $P < 0.05$ was considered statistically significant.

Results

The Protein Binding of DHC with Mouse Plasma and Heart. The ultrafiltration studies showed a high protein binding (PB: 88.50% ± 1.0%, Table 1) of DHC across the relevant plasma concentrations of 0.1–10 μM. The protein binding of DHC with the concentrations of 0.1–10 μM was 58.89% ± 8.6% in the heart. Quinidine (10 μM; PB: 74.01%) was used as a positive control, which is consistent with existing reports (Fremstad et al., 1979).

Dehydrocorydaline was Highly Concentrated in the Mouse Heart. The scope of this research was to explore the accumulation of DHC in the mouse heart after oral administration of *C. yanhusuo* extract (1.75 g·kg^{-1}) containing DHC (25 mg·kg^{-1}) or only DHC (25 mg·kg^{-1}) administration. DHC was rapidly distributed to the heart and reached a higher concentration, measured at 15 minutes, regardless of the substance administered (*C. yanhusuo* extract or DHC). The heart-to-plasma ratio ($K_{p,uu}$) of DHC was 603, 114, and 72 times at 15, 30, and 60 minutes after oral administration of *C. yanhusuo* extract (Table 2).

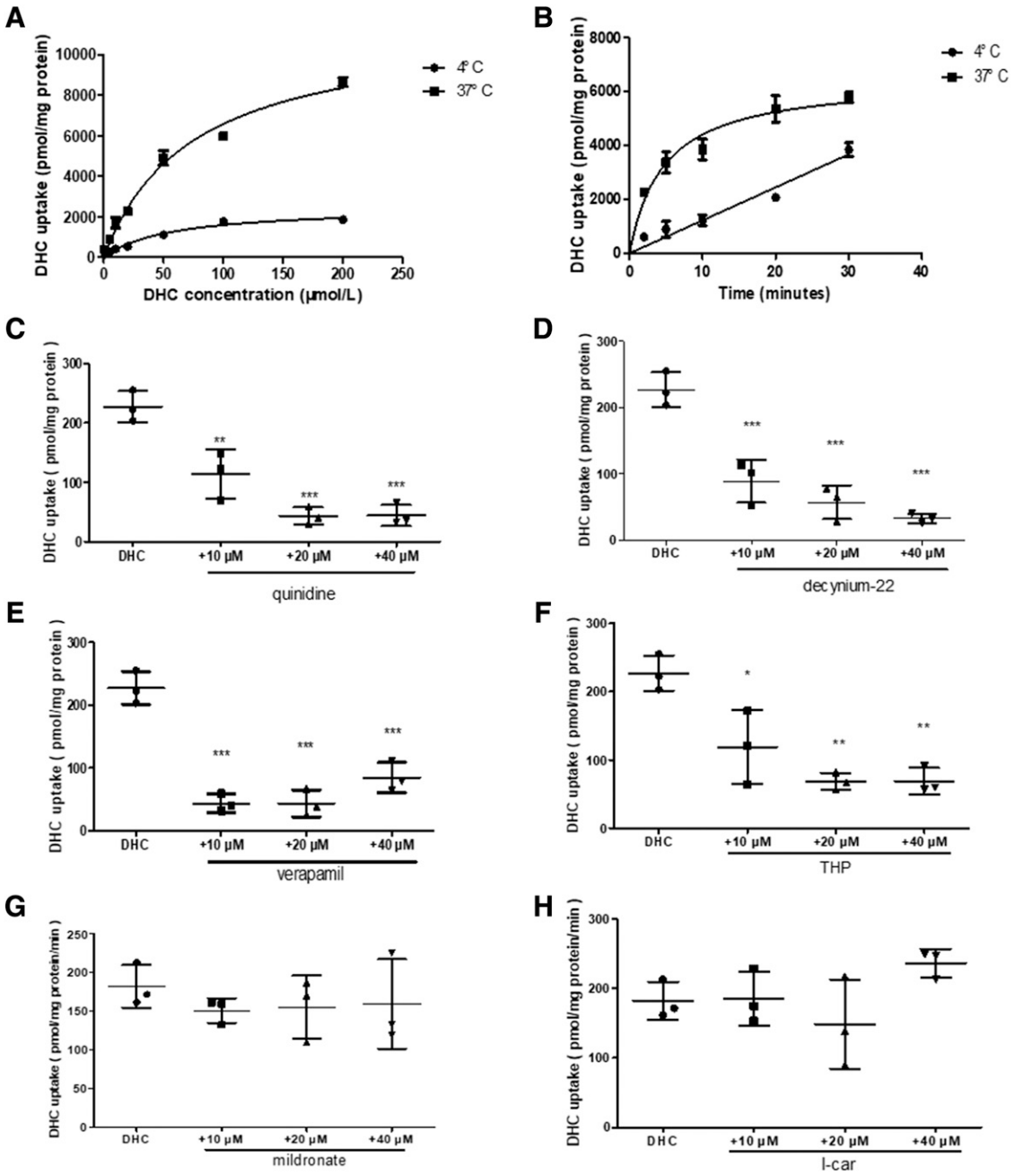

Fig. 5. OCT1/3 may participate in the accumulation of DHC in primary neonatal rat cardiomyocytes. Concentration-dependent (A) and time-dependent (B) accumulation of DHC at 4°C or 37°C. Effects of specific inhibitors, quinidine (C), decynium-22 (D), verapamil (E), THP (F), mildronate (G), and L-Car (H), on the accumulation of DHC at 37°C are shown. Data are presented as the means ± S.D., $n = 3$. Compared with the accumulation in cells treated without inhibitors at 37°C, $^{**}P < 0.01$; $^{***}P < 0.001$.

When the animals were administered DHC, the ratios at the same time points were 23, 146, and 37 times (Table 2). Importantly, the free concentrations of DHC in the heart were higher than the concentrations in the plasma.

***Oct1*, *Oct3*, *Octn1*, *Octn2,* and *PMAT* are Expressed in Mouse or Rat Heart.** We confirmed the expression levels of *Oct1*, *Oct3*, *Octn1*, *Octn2,* and *PMAT* mRNAs and proteins in the mouse and rat heart by using qRT-PCR (Fig. 2A) and Western blotting (Fig. 2, B and C) to study the mechanism of DHC uptake in the heart. The *Oct1*, *Oct3*, *Octn1*, and *Octn2* mRNAs were expressed at high levels in the mouse heart, whereas higher expression of *PMAT* mRNA was observed in the rat heart than in the mouse heart. Western blotting revealed the levels of OCT1, OCT3, OCTN1, and OCTN2 proteins in the mouse heart and PMAT protein in the rat heart. Liver tissue served as a positive control for each transporter protein.

Although *Oct1* mRNA expression was weak, Western blotting experiments (Supplemental Fig. 3) still revealed the expression levels of the OCT1 proteins in the rat heart.

DHC was a Substrate of OCT1 and OCT3 but Not of OCTN1, OCTN2, and PMAT. We evaluated the accumulation of DHC using transgenic cell models to identify the transporters that contributed to the transmembrane transport of DHC. As shown in Fig. 3, the accumulation of DHC in MDCK-hOCT1 and MDCK-hOCT3 cells was nearly 20-fold and 2.1-fold higher than in mock cells (Fig. 3, A and B). Nevertheless, these changes were suppressed by verapamil (100 μM, an inhibitor of OCT1) and decynium-22 (10 μM, an inhibitor of OCT3). Thus, DHC

TABLE 1

The protein binding of DHC with mouse plasma and heart (means ± S.D., n = 3) is presented

The protein binding of DHC with the concentrations of 0.1–10 μM were performed by an ultrafiltration method. The protein binding was determined as the protein binding (%) = 1−Cf/Ct × (1+P %), where Cf was the free concentration, Ct was the total concentration, and P% was the nonspecific binding of the centrifugal ultrafiltration device.

		Protein Binding (%)			
		Plasma	Mean	Heart	Mean
DHC	0.1 μM	89.66 ± 1.9	88.50 ± 1.0	66.72 ± 2.1	58.89 ± 8.6
	1 μM	88.17 ± 2.4		49.73 ± 8.4	
	10 μM	87.67 ± 1.1		60.21 ± 2.2	
Quinidine (10 μM)		74.01 ± 2.0		NA	

may be a substrate of OCT1 and OCT3. However, the accumulation of DHC was not altered in MDCK-hOCTN1/2 and MDCK-hPMAT cells compared with MDCK-mock cells (Fig. 3, C–E). Therefore, the Michaelis–Menten equation was further used to determine the typical dynamics of DHC in MDCK-hOCT1 and MDCK-hOCT3 cells. The K_m values were 11.29 ± 3.3 and 8.96 ± 3.7 μM, and V_{max} values were 3.314 ± 0.18 and 0.3558 ± 0.045 μmol/mg protein per minute in MDCK-hOCT1 and MDCK-hOCT3 cells (Fig. 4, A and C). The capacity of MDCK-hOCT1 cells to transport DHC was higher than MDCK-hOCT3 cells, with the C_{lint} (V_{max}/K_m) of 293.5 and 39.67 ml/mg protein per minute. Thus, DHC was a substrate of OCT1 and OCT3 but not OCTN1, OCTN2, or PMAT.

OCT1/3 May Participate in the Accumulation of Dehydrocorydaline in Primary Neonatal Rat Cardiomyocytes. The concentration- and time-dependent accumulation of DHC was analyzed in primary neonatal rat cardiomyocytes to further assess the carrier-mediated uptake of DHC in the heart. As shown in Fig. 5, A and B, DHC accumulated in cardiomyocytes at higher levels at 37°C than at 4°C. The results confirmed that transporters contribute to the transmembrane movement of DHC in primary neonatal rat cardiomyocytes. Furthermore, the accumulation of DHC in cardiomyocytes was inhibited by quinidine, decynium-22, THP, and verapamil but not mildronate and L-Car (Fig. 5, C–G). Quinidine, decynium-22, THP, and verapamil are selective inhibitors of OCT1/3, whereas mildronate and L-Car are selective inhibitors of OCTN2. Therefore, we speculate that OCT1 and OCT3 may contribute to the uptake of DHC in primary neonatal rat cardiomyocytes.

DHC is a Weak Substrate of MDR1. A statistical comparison of the P_{app} values in MDCK-mock and MDCK-MDR1 cells is presented in Table 3. The $P_{app\ (B\text{-}A)}$ and $P_{app\ (A\text{-}B)}$ values of DHC in MDCK-mock cells were 3.27×10^{-6} and 2.93×10^{-6} cm/s, implying that DHC displayed a moderate level of penetration. Regarding the transport of DHC, the ER in MDCK-MDR1 cells was higher than the corresponding values in MDCK-mock cells. Moreover, verapamil, a classic inhibitor of MDR1, inhibited efflux transport, and the efflux rate [ER = $P_{app\ (B\text{-}A)}$/$P_{app\ (A\text{-}B)}$] decreased from 1.71- to 0.86-fold. The transcellular transport of rhodamine 123 in MDCK-MDR1 cells produced an ER greater than 2.0-fold, indicating that the overexpression of P-gp in MDCK-MDR1 cells supported our experiment. The results described above showed that MDR1 might be related to DHC efflux transport in the cells.

Coadministration of THP Reduced the Accumulation of DHC in the Mouse Heart. THP, an inhibitor of OCT1 (IC_{50}: 13.9 ± 2.2 μM) and OCT3 (IC_{50}: 9.42 ± 0.37), was used for clarification of the OCT1/3 role in DHC uptake in the mouse heart. The concentration of THP in the heart was nearly 5165 ng/g (14.5 μM) 15 minutes after administration (Supplemental Table 3), whereas that of DHC (Fig. 6B) was approximately 40% lower than those in the control group treated with a similar DHC dose alone. The reduced accumulation of DHC in the heart may be attributed to the ability of THP to inhibit the functions of OCT1 and OCT3 in the mouse heart. However, the concentration of DHC in plasma was also reduced, potentially because of the increased concentrations of DHC in the liver and kidney (Fig. 6, C and D). Animal experiments further showed that THP decreased DHC uptake in the heart, possibly by inhibiting OCT1 and OCT3.

Discussion

Our studies elucidated DHC was highly concentrated in the mouse heart; OCT1/3 contributes to DHC accumulation in the heart; and THP, inhibitor of OCT1/3, could alter the distribution of DHC in the mouse heart.

A higher total concentration of DHC was observed in the mouse heart than in the mouse plasma after oral administration of *C. yanhusuo* extract or DHC. As direct measurement of free drug concentrations is challenging, it is typically obtained indirectly by measuring the protein binding and total drug concentration. The ultrafiltration studies showed a higher protein binding of DHC, across relevant concentrations of 0.1–10 μM (Table 1), in the plasma (PB = 88.50% ± 1.0%) than in the heart (PB = 58.89% ± 8.6%), revealing a high concentration of DHC in the mouse heart. The exact reasons for the differences between plasma and heart PB have not yet been identified, but we hypothesize that this may result from the different protein compositions in the plasma and

TABLE 2

Mean unbound concentrations of DHC in mouse plasma and heart after the oral administration of *C. yanhusuo* extract or DHC

The unbound concentrations of DHC in mouse plasma and heart was showed after the oral administration of *C.* yanhusuo extract (1.75 g·kg^{-1}) containing DHC (25 mg·kg^{-1}) or only DHC (25 mg·kg^{-1}). The unbound concentrations of DHC in the heart were significantly higher than the concentrations in the plasma. The data are shown as means ± S.D., n = 8. The $K_{p,uu}$ was described as the ratio of unbound tissue/unbound plasma concentration.

Time (min)	*C. Yanhusuo* Extract			DHC		
	Plasma (ng/ml)	Heart (ng/g)	Heart/ Plasma	Plasma (ng/ml)	Heart (ng/g)	Heart/ Plasma
15	0.8256 ± 1.2	497.9 ± 639	603	4.534 ± 3.8	104.1 ± 93	23
30	0.8872 ± 0.85	101.1 ± 94	114	0.1941 ± 0.12	28.42 ± 2.9	146
60	0.4612 ± 0.59	33.16 ± 22	72	0.9147 ± 1.2	34.26 ± 5.6	37

TABLE 3

Transcellular transport of DHC across MDCK-mock and MDCK-MDR1 cell monolayers

The data are shown as means ± S.D., n = 3. Unpaired Student's t test was used to compare the differences between two groups.

P_{app}	MDCK-mock ($\times 10^{-6}$ cm/s)			MDCK-MDR1 ($\times 10^{-6}$ cm/s)		
	AP-BL	BL-AP	ER	AP-BL	BL-AP	ER
DHC	2.93 ± 0.71	3.27 ± 0.19	1.12	3.46 ± 0.66	5.92 ± 0.32	1.71[a]
DHC + verapamil	3.18 ± 0.68	3.40 ± 0.25	1.07	2.95 ± 0.27	2.53 ± 0.23	0.86[b]
Rhodamine 123	1.99 ± 0.11	1.83 ± 0.23	0.92	1.06 ± 0.54	2.50 ± 0.03	2.36[a]

[a] $P < 0.01$ vs. ER of DHC in MDCK.
[b] $P < 0.01$ vs. ER of DHC in MDCK-MDR1.

heart. Albumin and acid glycoprotein, which account for 60% of the total plasma protein content, are the main sites for plasma drug-protein binding. The combination of drugs and plasma proteins affects the distribution, transport speed, action intensity, and elimination rate of the drug in the body.

In this study, the expression of *Oct1* mRNA and protein was observed in the mouse heart, and this is consistent with previous studies that have reported *Oct1* mRNA expression in the human heart (Koepsell, 2013). The amino acids of the OCT1 protein are 82%–96% similar in all species (Burckhardt and Wolff, 2000). Although transporters are expressed at lower levels in the heart than in the liver, several transporters have been reported to be expressed in the human heart, such as OCT3, OCTNs, organic anion transporting polypeptide 2B1, monocarboxylate transporter, and concentrative and equilibrative nucleoside transporters (Zhu et al., 2010; Solbach et al., 2011; Kou et al., 2018; Tzvetkov et al., 2018; Sun et al., 2019). OCT3 was expressed in human cardiomyocytes and vascular endothelial cells (Klaassen and Aleksunes, 2010; Solbach et al., 2011). These transporters also play important roles in maintaining the homeostasis of cardiac metabolism and function. Considering the structural characteristics of DHC and its presence as a cation under physiologic conditions, we only considered OCTs, OCTNs, and PMAT transporters in the present study.

OCTs have been widely recognized as one of the factors in drug disposition and drug-drug/herb interactions. For example, in Oct3 knockout mice (Zwart et al., 2001), the accumulation of MPP^+ (a classic substrate of OCT3) was markedly reduced in the heart. In this study, DHC was taken up partly by OCT1 and OCT3 in the transgenic cells (Fig. 3, A and B). Moreover, DHC inhibited OCT1 and OCT3 at low IC_{50} values of 7.736 ± 0.56 and 1.326 ± 1.0 μM, respectively (Supplemental Fig. 4). Besides, the accumulation of DHC in primary neonatal rat cardiomyocytes was inhibited by quinidine, decynium-22, and THP, which were positively correlated with the concentrations (Fig. 5,

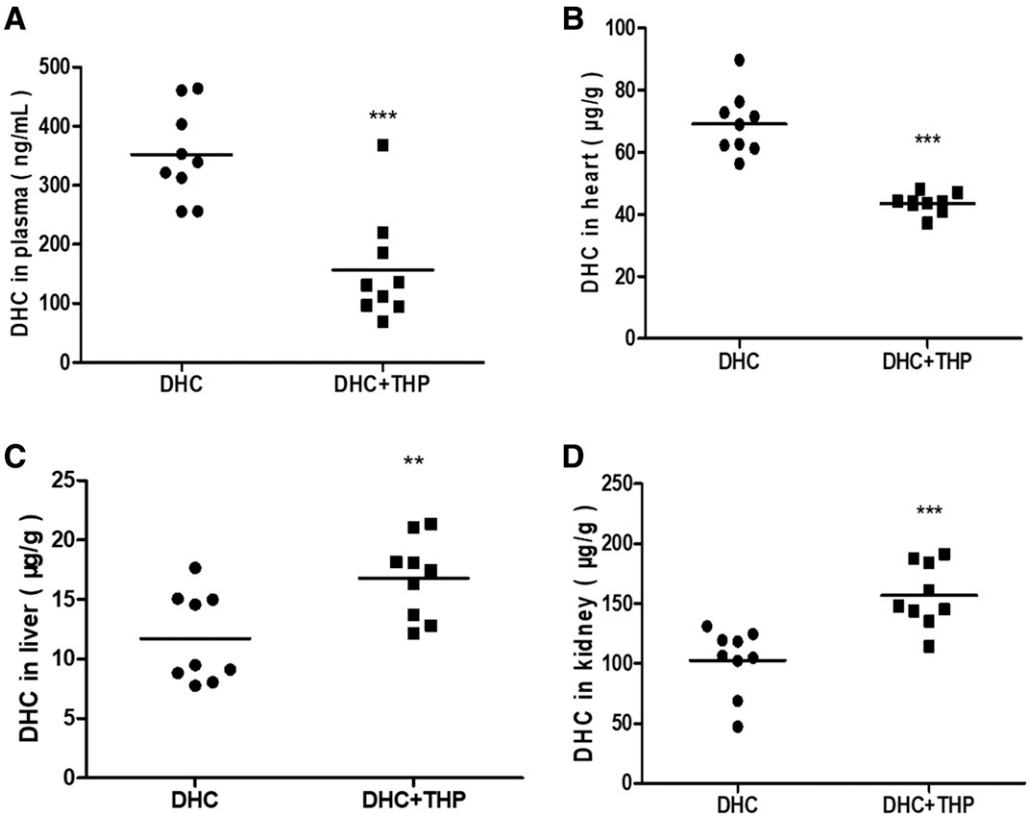

Fig. 6. THP could decrease the concentrations of DHC in the plasma and heart. ICR mice were treated with a single tail vein injection of DHC or a combination of THP and DHC, and the DHC concentrations in plasma (A), heart (B), liver (C), and kidney (D) were identified and evaluated. The sample sizes did not change during the experiment. Each symbol shows data from an individual mouse. The lines show the group means. The analyses steps were decided before we looked at the data to avoid bias. Data are presented as the means ± S.D., $n = 9$. Compared with the DHC group, $^{**}P < 0.01$; $^{***}P < 0.001$.

C–E). The uptake of DHC was less inhibited at 40 μM verapamil compared with 10 and 20 μM. This may be because the higher concentration of verapamil also inhibited the function of the efflux transporter, resulting in a reduction in the efflux of intracellular DHC. Regrettably, there were no specific inhibitors (Supplemental Table 2). Multiple inhibitors were comprehensively employed in various cell models and primary cells to reasonably conclude that OCT1/3 may contribute to DHC uptake in the mouse heart.

The administration of a tail vein injection instead of oral administration was conducted in mice to simplify the study on the effect of OCT on the cardiac transport of DHC. We found a higher unbound concentration of DHC in the heart after oral administration than in plasma. We also found the heart/plasma ratio of concentration of DHC varies greatly with time (Table 2); intravenous injection can ensure that the inhibitor THP can quickly reach the heart tissue and avoid the intestinal absorption and liver metabolism. As predicted, THP reduced DHC uptake in the heart by inhibiting OCT1 and OCT3. Although THP was also an inhibitor of MDR1, it exerted a weaker inhibitory effect on MDR1, with an IC_{50} (20–40 μM) that was higher than the IC_{50} of OCT1 (13.9 ± 2.2 μM) (Sun et al., 2012; Tu et al., 2013). Therefore, our experiments showed the importance of OCT1/3 in DHC uptake in the heart. However, the concentrations of DHC in the liver and kidney were higher than those in animals that were not treated with THP (Fig. 6, C and D). Howbeit, the exact explanations for this accumulation have not been elucidated. We speculate that the accumulation in these tissues may be attributed to other complex factors, such as liver metabolism and renal excretion. THP inhibits the activity of CYP2D6 (IC_{50} 3.04 ± 0.26 μM) and CYP3A4 in the liver (Zhao et al., 2012, 2016; Sun et al., 2013); therefore, one of the potential explanations for the increased concentration of DHC in the liver is that THP exerts a greater inhibitory effect on cytochrome P450s than on OCTs.

In summary, transporters contribute to the distribution of DHC in the mouse heart. DHC may be accumulated in part by OCT1/3 and excreted by MDR1 in the heart. THP, an inhibitor of OCT1/3, could alter the distribution of DHC in the mouse heart.

Acknowledgments

We thank Dr. Peihua Luo and Kui Zeng for helping with experiments, and we thank Haihong Hu for managing instruments.

Authorship Contributions

Participated in research design: Chen, Jiang, Zeng, Zhou.
Conducted experiments: Chen, Li, Yi, Du.
Performed data analysis: Chen, Jiang, Zhou.
Wrote or contributed to the writing of the manuscript: Chen, Jiang, Zhou.

References

Bai M, Ma Z, Sun D, Zheng C, Weng Y, Yang X, Jiang T, and Jiang H (2017) Multiple drug transporters mediate the placental transport of sulpiride. *Arch Toxicol* **91**:3873–3884.
Bexten M, Oswald S, Grube M, Jia J, Graf T, Zimmermann U, Rodewald K, Zolk O, Schwantes U, Siegmund W, et al. (2015) Expression of drug transporters and drug metabolizing enzymes in the bladder urothelium in man and affinity of the bladder spasmolytic trospium chloride to transporters likely involved in its pharmacokinetics. *Mol Pharm* **12**:171–178.
Burckhardt G and Wolff NA (2000) Structure of renal organic anion and cation transporters. *Am J Physiol Renal Physiol* **278**:F853–F866.
Dambrova M, Skapare-Makarova E, Konrade I, Pugovics O, Grinberga S, Tirzite D, Petrovska R, Kalvins I, and Liepins E (2013) Meldonium decreases the diet-increased plasma levels of trimethylamine N-oxide, a metabolite associated with atherosclerosis. *J Clin Pharmacol* **53**: 1095–1098.
Dou Z, Li K, Wang P, and Cao L (2012) Effect of wine and vinegar processing of Rhizoma Corydalis on the tissue distribution of tetrahydropalmatine, protopine and dehydrocorydaline in rats. *Molecules* **17**:951–970.
Du W, Jin L, Li L, Wang W, Zeng S, Jiang H, and Zhou H (2018) Development and validation of a HPLC-ESI-MS/MS method for simultaneous quantification of fourteen alkaloids in mouse plasma after oral administration of the extract of corydalis yanhusuo tuber: application to pharmacokinetic study. *Molecules* **23**:714.
Fraser-Spears R, Krause-Heuer AM, Basiouny M, Mayer FP, Manishimwe R, Wyatt NA, Dobrowolski JC, Roberts MP, Greguric I, Kumar N, et al. (2019) Comparative analysis of novel decynium-22 analogs to inhibit transport by the low-affinity, high-capacity monoamine transporters, organic cation transporters 2 and 3, and plasma membrane monoamine transporter. *Eur J Pharmacol* **842**:351–364.
Fremstad D, Nilsen OG, Storstein L, Amlie J, and Jacobsen S (1979) Pharmacokinetics of quinidine related to plasma protein binding in man. *Eur J Clin Pharmacol* **15**:187–192.
Fujii T, Miyazaki H, Nambu K, Kagemoto A, and Hashimoto M (1984) [Disposition and metabolism of 14C-dehydrocorydaline in mice and rats]. *Radioisotopes* **33**:519–525.
Grube M, Ameling S, Noutsias M, Köck K, Triebel I, Bonitz K, Meissner K, Jedlitschky G, Herda LR, Reinthaler M, et al. (2011) Selective regulation of cardiac organic cation transporter novel type 2 (OCTN2) in dilated cardiomyopathy. *Am J Pathol* **178**:2547–2559.
Guan H, Li K, Wang X, Luo X, Su M, Tan W, Chang X, and Shi Y (2017) Identification of metabolites of the cardioprotective alkaloid dehydrocorydaline in rat plasma and bile by liquid chromatography coupled with triple quadrupole linear ion trap mass spectrometry. *Molecules* **22**: 1686.
Hausner EA, Elmore SA, and Yang X (2019) Overview of the components of cardiac metabolism. *Drug Metab Dispos* **47**:673–688.
Huang JY, Fang M, Li YJ, Ma YQ, and Cai XH (2010) [Analgesic effect of Corydalis yanhusuo in a rat model of trigeminal neuropathic pain]. *Nan Fang Yi Ke Da Xue Xue Bao* **30**:2161–2164.
Iranshahy M, Quinn RJ, and Iranshahi M (2014) Biologically active isoquinoline alkaloids with drug-like properties from the genus Corydalis. *RSC Advances* **4**:15900–15913.
Kamal MA, Jiang H, Hu Y, Keep RF, and Smith DE (2009) Influence of genetic knockout of Pept2 on the in vivo disposition of endogenous and exogenous carnosine in wild-type and Pept2 null mice. *Am J Physiol Regul Integr Comp Physiol* **296**:R986–R991.
Klaassen CD and Aleksunes LM (2010) Xenobiotic, bile acid, and cholesterol transporters: function and regulation. *Pharmacol Rev* **62**:1–96.
Koepsell H (2013) The SLC22 family with transporters of organic cations, anions and zwitterions. *Mol Aspects Med* **34**:413–435.
Koepsell H (2020) Organic cation transporters in health and disease. *Pharmacol Rev* **72**:253–319.
Koepsell H, Lips K, and Volk C (2007) Polyspecific organic cation transporters: structure, function, physiological roles, and biopharmaceutical implications. *Pharm Res* **24**:1227–1251.
Kou L, Sun R, Ganapathy V, Yao Q, and Chen R (2018) Recent advances in drug delivery via the organic cation/carnitine transporter 2 (OCTN2/SLC22A5). *Expert Opin Ther Targets* **22**: 715–726.
Li L, Sun S, Weng Y, Song F, Zhou S, Bai M, Zhou H, Zeng S, and Jiang H (2016) Interaction of six protoberberine alkaloids with human organic cation transporters 1, 2 and 3. *Xenobiotica* **46**: 175–183.
Li L, Tu M, Yang X, Sun S, Wu X, Zhou H, Zeng S, and Jiang H (2014) The contribution of human OCT1, OCT3, and CYP3A4 to nitidine chloride-induced hepatocellular toxicity. *Drug Metab Dispos* **42**:1227–1234.
Li P, Ren J, Duan C, Lin C, and Liu J (2010) [Effects of four components of Rhizoma Corydalis on anoxia and peroxidation injuries in neonatal cardiomyocytes]. *Zhongguo Zhongyao Zazhi* **35**: 84–88.
Liu YY, Wang TX, Zhou JC, Qu WM, and Huang ZL (2019) Dopamine D_1 and D_2 receptors mediate analgesic and hypnotic effects of l-tetrahydropalmatine in a mouse neuropathic pain model. *Psychopharmacology (Berl)* **236**:3169–3182.
Ma Z, Yang X, Jiang T, Bai M, Zheng C, Zeng S, Sun D, and Jiang H (2017) Multiple SLC and ABC transporters contribute to the placental transfer of entecavir. *Drug Metab Dispos* **45**: 269–278.
Smith DA, Di L, and Kerns EH (2010) The effect of plasma protein binding on in vivo efficacy: misconceptions in drug discovery. *Nat Rev Drug Discov* **9**:929–939.
Solbach TF, Grube M, Fromm MF, and Zolk O (2011) Organic cation transporter 3: expression in failing and nonfailing human heart and functional characterization. *J Cardiovasc Pharmacol* **58**: 409–417.
Sun S, Chen Z, Li L, Sun D, Tian Y, Pan H, Bi H, Huang M, Zeng S, and Jiang H (2012) The two enantiomers of tetrahydropalmatine are inhibitors of P-gp, but not inhibitors of MRP1 or BCRP. *Xenobiotica* **42**:1197–1205.
Sun S, Wang K, Lei H, Li L, Tu M, Zeng S, Zhou H, and Jiang H (2014) Inhibition of organic cation transporter 2 and 3 may be involved in the mechanism of the antidepressant-like action of berberine. *Prog Neuropsychopharmacol Biol Psychiatry* **49**:1–6.
Sun S, Zhou S, Lei S, Zhu S, Wang K, Jiang H, and Zhou H (2019) Jatrorrhizine reduces 5-HT and NE uptake via inhibition of uptake-2 transporters and produces antidepressant-like action in mice. *Xenobiotica* **49**:1237–1243.
Sun SY, Wang YQ, Li LP, Wang L, Zeng S, Zhou H, and Jiang HD (2013) Stereoselective interaction between tetrahydropalmatine enantiomers and CYP enzymes in human liver microsomes. *Chirality* **25**:43–47.
Tan CN, Zhang Q, Li CH, Fan JJ, Yang FQ, Hu YJ, and Hu G (2019) Potential target-related proteins in rabbit platelets treated with active monomers dehydrocorydaline and canadine from Rhizoma corydalis. *Phytomedicine* **54**:231–239.
Tu M, Sun S, Wang K, Peng X, Wang R, Li L, Zeng S, Zhou H, and Jiang H (2013) Organic cation transporter 1 mediates the uptake of monocrotaline and plays an important role in its hepatotoxicity. *Toxicology* **311**:225–230.
Tzvetkov MV, Matthaei J, Pojar S, Faltraco F, Vogler S, Prukop T, Seitz T, and Brockmöller J (2018) Increased systemic exposure and stronger cardiovascular and metabolic adverse reactions to fenoterol in individuals with heritable OCT1 deficiency. *Clin Pharmacol Ther* **103**:868–878.
Vandergriff AC, Hensley MT, and Cheng K (2015) Isolation and cryopreservation of neonatal rat cardiomyocytes. *J Vis Exp* **98**:52726.
Wei F, Hu Q, Huang J, Han S, and Wang S (2017) Screening active compounds from Corydalis yanhusuo by combining high expression VEGF receptor HEK293 cell membrane chromatography with HPLC - ESI - IT - TOF - MSn method. *J Pharm Biomed Anal* **136**:134–139.
Weng YY, Jin LS, Wang YQ, Song FF, Li LP, Zhou H, Zeng S, and Jiang HD (2016) [Establishment and application of cell models with stable expression of hOCTN1/2]. *Yao Xue Xue Bao* **51**:931–937.
Wu H, Waldbauer K, Tang L, Xie L, McKinnon R, Zehl M, Yang H, Xu H, and Kopp B (2014) Influence of vinegar and wine processing on the alkaloid content and composition of the traditional Chinese medicine Corydalis Rhizoma (Yanhusuo). *Molecules* **19**:11487–11504.
Yang J, Sambandam N, Han X, Gross RW, Courtois M, Kovacs A, Febbraio M, Finck BN, and Kelly DP (2007) CD36 deficiency rescues lipotoxic cardiomyopathy. *Circ Res* **100**: 1208–1217.

Yang XB, Yang XW, and Liu JX (2014) [Study on material base of corydalis rhizoma]. *Zhongguo Zhongyao Zazhi* **39**:20–27.
Yu L, Shen Q, Zhou Q, Jiang H, Bi H, Huang M, Zhou H, and Zeng S (2013) In vitro characterization of ABC transporters involved in the absorption and distribution of liensinine and its analogs. *J Ethnopharmacol* **150**:485–491.
Zeng Q, Bai M, Li C, Lu S, Ma Z, Zhao Y, Zhou H, Jiang H, Sun D, and Zheng C (2019) Multiple drug transporters contribute to the placental transfer of emtricitabine. *Antimicrob Agents Chemother* **63**:e00199-19.
Zhang D, Hop CECA, Patilea-Vrana G, Gampa G, Seneviratne HK, Unadkat JD, Kenny JR, Nagapudi K, Di L, Zhou L, et al. (2019) Drug concentration asymmetry in tissues and plasma for small molecule-related therapeutic modalities. *Drug Metab Dispos* **47**:1122–1135.
Zhang Y and Benet LZ (1998) Characterization of P-glycoprotein mediated transport of K02, a novel vinylsulfone peptidomimetic cysteine protease inhibitor, across MDR1-MDCK and Caco-2 cell monolayers. *Pharm Res* **15**:1520–1524.
Zhao X, Tang H, Wang YJ, Yu X, Liu Y, Zhang J, Qin J, and Guo SF (2003) [The influence of dehydrocorydaline on intracellular free calcium concentration during hypoxia in myocardial cell of Guinea-pigs]. *Zhongguo Ying Yong Sheng Li Xue Za Zhi* **19**:222–225.
Zhao Y, Hellum BH, Liang A, and Nilsen OG (2012) The in vitro inhibition of human CYP1A2, CYP2D6 and CYP3A4 by tetrahydropalmatine, neferine and berberine. *Phytother Res* **26**:277–283.
Zhao Y, Liang A, Zhang Y, Li C, Yi Y, and Nilsen OG (2016) Impact of tetrahydropalmatine on the pharmacokinetics of probe drugs for CYP1A2, 2D6 and 3A isoenzymes in beagle dogs. *Phytother Res* **30**:906–914.
Zhu HJ, Appel DI, Gründemann D, and Markowitz JS (2010) Interaction of organic cation transporter 3 (SLC22A3) and amphetamine. *J Neurochem* **114**:142–149.
Zwart R, Verhaagh S, Buitelaar M, Popp-Snijders C, and Barlow DP (2001) Impaired activity of the extraneuronal monoamine transporter system known as uptake-2 in Orct3/Slc22a3-deficient mice. *Mol Cell Biol* **21**:4188–4196.

Address correspondence to: Hui Zhou, Laboratory of Pharmaceutical Analysis and Drug Metabolism, College of Pharmaceutical Sciences, Zhejiang University, 866 Yuhangtang Road, Hangzhou 310058, China. E-mail: zhouhui@zju.edu.cn